Pharmaceutical Research (2022) 39:2147–2162
https://doi.org/10.1007/s11095-022-03324-9

ORIGINAL ARTICLE

Mechanistic Study on the Effect of Renal Impairment on the Pharmacokinetics of Vildagliptin and its Carboxylic Acid Metabolite

Zitao Guo[1,2] · Fandi Kong[2,3] · Ningjie Xie[2,3] · Zhendong Chen[2] · Jiafeng Hu[2,3] · Xiaoyan Chen[1,2,3]

Received: 1 March 2022 / Accepted: 24 June 2022 / Published online: 6 July 2022

Abstract

Purpose To clarify the mechanism of renal impairment leading to different degrees of increased plasma exposure to dipeptidyl peptidase 4 inhibitor vildagliptin and its major metabolite, M20.7.

Methods The 5/6 nephrectomized (5/6 Nx) rat model, to simulate chronic renal failure (CRF) patients, combined with kidney slices and transporter studies in vitro were used to assess this pharmacokinetic differences.

Results After intragastric administration to 5/6 Nx rats, vildagliptin showed increased plasma levels by 45.8%, and M20.7 by 7.51 times, which was similar to patients with severe renal impairment. The recovery rate of M20.7 in urine and feces increased by less than 20%, showing limited effect of renal impairment on vildagliptin metabolism. In vitro studies found M20.7 to be the substrate for organic anion transporter 3 (OAT3). However, the active uptake of M20.7 in renal slices showed no difference between the 5/6 Nx and normal rats. In OAT3 overexpressed cells, the protein-bound uremic toxins, 3-carboxy-4-methyl-5propyl-2-furanpropionate (CMPF), hippuric acid (HA) and indoxyl sulfate (IS), which accumulate in CRF patients, inhibited M20.7 uptake with IC_{50} values of 5.75, 29.0 and 69.5 μM respectively, far lower than plasma concentrations in CRF patients, and showed a mixed inhibition type.

Conclusions The large increase in plasma exposure of M20.7 could be attributed to the accumulation of uremic toxins in CRF patients, which inhibited OAT3 activity and blocked renal excretion of M20.7, while vildagliptin, with high permeability, showed a slight increase in plasma exposure due to reduced glomerular filtration.

Keywords Vildagliptin carboxylic acid metabolite M20.7 · Renal impairment · Pharmacokinetics · Uremic toxins · Transporter inhibition

Introduction

Vildagliptin (Fig. 1) is a potent, selective dipeptidyl peptidase IV (DPP-IV) inhibitor developed by Novartis [1]. Clinically, it can be used alone or in combination with metformin for the treatment of type 2 diabetes. DPP-IV is a transmembrane cell surface aminopeptidase, which is widely expressed in liver, kidney, lung, intestine and other tissues, as well as capillary endothelial cells and subsets of T lymphocytes. DPP-IV also exists in a soluble form in the plasma and other body fluids where it can maintain full enzymatic activity [2]. DPP-IV can rapidly inactivate insulin-like glucagon-like peptide 1 (GLP-1) and glucose-dependent insulin polypeptide (GIP), which are both indispensable components involved in the physiological control of insulin release and the regulation of blood glucose [3]. At present, cyanopyrrolidine DPP-IV enzyme inhibitors, such as vildagliptin, saxagliptin and alogliptin, represent the first drugs to be developed whereby renal excretion is the principal clearance pathway.

Vildagliptin is mainly metabolized into the carboxylic acid metabolite M20.7 (Fig. 1, 1-[2-(3-hydroxyadamantan-1-ylamino)

Zitao Guo and Fandi Kong contributed equally to this work.

✉ Xiaoyan Chen
xychen@simm.ac.cn

1 School of Environmental Chemistry and Engineering, Shanghai University, 99 Shangda Road BaoShan District, Shanghai 200444, China

2 Shanghai Institute of Materia Medica, Chinese Academy of Sciences, 501 Haike Road, Shanghai 201203, China

3 University of Chinese Academy of Sciences, Beijing 100049, China

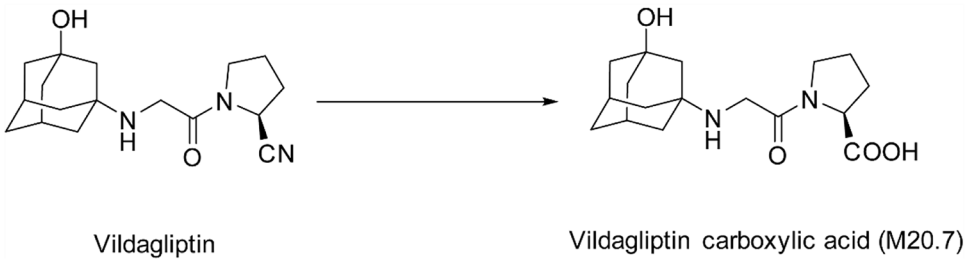

Fig. 1 Major metabolic pathways of vildagliptin in humans

acetyl]pyrrolidine-2(S)-carboxylic acid) through cyanide hydrolysis catalyzed by DPPs in humans, where the urine recovery rates of the parent drug and M20.7 were 23% and 50%, respectively [4, 5]. It has been reported that in patients with mild, moderate, and severe chronic renal failure (CRF) and end-stage renal disease (ESRD), the areas under the plasma concentration-time curves (AUC) for vildagliptin increased by 32% to 134%, and the maximum plasma concentration (C_{max}) increased by 8% to 66%, while the AUC for M20.7 increased by 1.6 to 6.7 times [6]. The effect of renal impairment on the pharmacokinetics of the metabolite M20.7 was significantly higher than that of the parent drug.

Similar to vildagliptin, DPP4 inhibitors saxagliptin and alogliptin, mainly excreted by kidney, also exhibited increased plasma exposures in CRF and ESRD patients. Therefore, it is recommended that the dose should be halved or not recommended at all in some patients [7, 8]. The mechanism involved in the pharmacokinetic changes of these drugs in patients with renal impairment has not been reported. Therefore, in this study, vildagliptin a commonly used drug was selected to explore these mechanisms.

Multiple causes have been reported to result in the changes in pharmacokinetics of the drugs and/or metabolites in patients with CRF, such as decreased glomerular filtration rate, abnormal plasma protein binding and decreased expression and activity of transporters and enzymes, etc. [9–11]. Recently, several studies have shown that some uremic toxins accumulated in patients with renal failure can inhibit the active renal uptake of drugs or metabolites, which in turn blocks their renal excretion, resulting in increased plasma exposures [12–14]. Protein-bound uremic toxins, such as 3-carboxy-4-methyl5-propyl-2-furanpropionate (CMPF), hippuric acid (HA), indoxyl sulfate (IS) and indole-3-acetic acid (IAA), cannot be effectively removed from the body due to tight binding to serum albumin. The concentrations of such uremic toxins in CRF patients can reach 10 to nearly 100 times that seen in the healthy population [15]. It has been reported that CMPF and HA can inhibit the renal uptakes of the OAT1 substrates adefovir and tenofovir, and the OAT3 substrates famotidine and the conjugated metabolites of morindazole, with IC_{50} values lower than their plasma concentrations in CRF patients, which may explain the changes in the pharmacokinetics of these substrates in these patients [13, 16, 17]. Since M20.7 but not vildagliptin, as a carboxylic acid metabolite, has low membrane permeability and all ionization under physiological conditions (evaluated by ACD/ChemSketch), we speculate that transporters may be responsible for M20.7 into the kidney. The inhibitory effect of uremic toxins on the transporters involved in the excretion of M20.7 may be the possible mechanism for the significant increase of M20.7 exposure in CRF patients.

The 5/6 Nx rat model is the most widely used in progressive CRF studies due to hyperfiltration, hyperperfusion, and hypertension leading to renal insufficiency in the remaining nephrons [18]. Similar to CRF humans, the levels of uremic toxins IS and HA were significantly increased in 5/6 Nx rats [19]. In addition, it was found that a decrease in protein (40%) and mRNA (75%) expression for Oat1 as well as reduced protein (87%) and mRNA (70%) expression for Oat3 in the kidneys of 5/6 Nx rat [20]. Therefore, 5/6 Nx rat is also a suitable animal model to study the effect of renal insufficiency on pharmacokinetics.

To elucidate the potential mechanisms of renal impairment leading to different degrees of increased plasma exposure to vildagliptin and M20.7, the 5/6 Nx rat model was employed to mimic CRF patients for comparing the pharmacokinetics of vildagliptin and M20.7 in control and 5/6 Nx rats, as well as the metabolism of vildagliptin. Next, renal active uptake of M20.7 was examined using kidney slices. Subsequently, renal uptake transporters overexpressed human embryonic kidney 293 (HEK293) cells were used to identify the transporters involved in the M20.7 uptake. Finally, the correlation between the concentration of uremic toxins and exposure to vildagliptin and M20.7 in rats was evaluated, and then the potential effect of uremic toxins on the renal uptake of M20.7 was examined on the kidney slices and transporter transfected HEK293 cells.

Materials and Methods

Chemicals and Reagents

Vildagliptin and salicylic acid were purchased from Meilun Biology Technology (Dalian, China). Vildagliptin carboxylic acid metabolite M20.7 was purchased from Phystandard biotech Co., Ltd. (Shenzhen, China). Internal standard compounds besigliptin and besigliptin carboxylic acid metabolite were

kindly provided by Jiangsu Hengrui Medicine Co., Ltd. (Lianyungang, China). Estrone-3-sulfate (E3S), para-amino hippuric acid (PAH), 1-methyl-4-phenyl pyridine ion (MPP+), probenecid, tetraethylammonium (TEA), Hanks' balanced salt solution (HBSS), Indoxyl sulfate potassium salt (IS) were obtained from SigmaAldrich (St. Louis, MO). d5-E3S, d3-MPP+, d4-PAH, and CMPF were purchased from Toronto Research Chemicals (North York, ON, Canada). HA and indole-3-acetate acid (IAA) were supplied by J&K Scientific (Beijing, China). TRIzol reagent, diethylpyrocarbonate–treated water, Dulbecco's modified Eagles medium (DMEM), fetal bovine serum, 0.05% trypsin-EDTA, penicillin G, streptomycin, and SuperScript III reverse transcriptase kit were purchased from Invitrogen (Carlsbad, CA). The BCA protein assay kit was purchased from Beyotime (Jiangsu, China). Assay kits of creatinine, urine protein, and blood urea nitrogen (BUN) were supplied by Nanjing Jiancheng Bioengineering Institute (Jiangsu, China). Deionized water was obtained using a Millipore Milli-Q gradient water purification system (Molsheim, France). The inorganic salts used for the preparation of buffers were purchased from the China National Medicines Co., Ltd. (Beijing, China). All other solvents and reagents were of either high-performance liquid chromatography or analytic grade.

Construction of the 5/6 Nx Rat Model

All procedures involving animals were carried out based on the *Guide for the Care and Use of Laboratory Animals* of the Shanghai Institute of Materia Medica, Chinese Academy of Sciences.

The 5/6 Nx rat model was established using the two-step method as previously described [21]. After the rats were anesthetized by intraperitoneal injection of pentobarbital sodium (50 mg/kg), the renal parenchyma of the upper and lower poles was removed. After suturing, the rats were fed for 1 week, and then after anesthesia as above, the whole right kidney was removed. The control group was treated the same as that of the 5/6 Nx group except that the kidney was not removed. Rats were free to drink water after the operation, but to limit the effect of CRF-induced malnutrition in later experiments, the rats in the control group were fed with the amount of food given the day before in the 5/6 Nx group.

On the 41st day after nephrectomy, the rats were placed in a metabolic cage to collect urine for 24 h and to determine urinary protein and creatinine clearance. Blood samples were taken from the intraocular venous plexus, and then left to stand for 30 min, before centrifuging at 11000 g and 4°C for 5 min, and then the serum creatinine and urea nitrogen were detected.

Using the corresponding assay kits to measure urine creatinine and protein, serum creatinine, and BUN following the manufacturer's instructions.

Rat Pharmacokinetic Experiments

The animals were fasted for 12 h but allowed to drink water freely before experiments. The rats in the 5/6 Nx group ($n=9$) and the control group ($n=5$) were given 10 mg/kg vildagliptin by intragastric administration and blood samples were collected before dosing (0 h), at 10, 20, 40 min and at 1, 1.5, 2, 3, 5, 7, 10 and 24 h post-dosing. Plasma samples were centrifuged at 11,000 g for 5 min at 4°C. After the completion of the pharmacokinetic experiments, the rats were anesthetized with pentobarbital sodium and bled from the abdominal aorta. The residual kidney tissue from the 5/6 Nx group and the left kidney of the control group were removed and frozen with liquid nitrogen and then stored at −80°C.

The rats in the 5/6 Nx ($n=7$) and the control groups ($n=5$) were injected with M20.7 via the tail vein at a dose of 1.5 mg/kg, respectively. The blood samples were collected before the dose (0 h), at 5, 15, 30, 45 min and 1, 1.5, 2, 3, 5, 7, 10 h after administration. Plasma samples were harvested as described above.

Rat Excretion Experiments

The animals were placed into metabolic cages, fasted for 12 h before administration of vildagliptin, and were allowed to drink freely. Rats in the 5/6 Nx ($n=4$) and control groups ($n=4$) were given 10 mg/kg vildagliptin. Urine and fecal samples were collected at 0–4 h, 4–8 h, 8–12 h, 12–24 h, 24–48 h, 48–70 h, and 70–96 h. The volume of urine and the fecal sample weights from each period were measured and stored at −80°C.

In Vitro Metabolism of Vildagliptin

The effect of chronic renal impairment on the metabolism of vildagliptin in the liver and kidney was investigated. Liver and kidney homogenates from control ($n=3$) and the 5/6 Nx group ($n=3$) were prepared [22]. After the rats were anesthetized with pentobarbital sodium, the abdominal aorta was bled, and the liver and kidneys were quickly washed with ice-cold normal saline, frozen in liquid nitrogen, and stored at −80°C. An appropriate amount of liver and kidney tissue was cut on ice and homogenized with cold 100 mM phosphate buffer saline (PBS, pH 7.4) containing 0.5 mM $MgCl_2$. After homogenization, the liver and kidney homogenates from each rat were normalized for protein content by adjusting with PBS. The total volume of the incubation system was 200 μL, and the medium was PBS, which included vildagliptin at a final concentration of 0.05 μM, 0.30 μM and 2.00 μM, liver/kidney homogenate with 4 mg/mL protein concentration, and in the presence or absence of saxagliptin (DPP IV inhibitor) at 20 μM [5]. The incubation time was

3 h and the reaction was terminated with the same volume of ice-cold acetonitrile. The samples were then stored at −80°C and the production of M20.7 was determined by liquid chromatography with tandem mass spectrometry (LC-MS/MS).

Uptake Studies Using Transporter-Expressing HEK293 Cells

Vildagliptin and M20.7 uptake by OA1, OAT3, and OCT2 was evaluated using transporter-transfected cell lines as previously described with slight modification [23]. The transporters (OAT1, OAT3, or OCT2) were transfected into HEK293 cells and empty-vector-transfected control cells (mock) were all constructed at HD Bioscience (Shanghai, China). The functions of the transporters in these cells were assessed using corresponding positive substrates and inhibitors. PAH (40 μM, OAT1), and E3S (5 μM, OAT3), and MPP (5 μM, OCT2) were used as substrates for the transporters. In addition, the inhibitors of each transporter were selected as follows: probenecid (200 μM, OAT1 and OAT3), and TPA (200 μM, OCT2). Cells were cultured in Dulbecco's Modified Eagle's Medium supplemented with 10% fetal bovine serum, 100 units/ml of penicillin G, 100 mg/ml of streptomycin at 37°C in a humidified 5% CO_2 atmosphere. When the cell growth was sub-confluent, the cells were digested with 0.05% trypsin, then seeded into 24-well plates that had been coated with D-polylysine (Poly-D-Lysine, PDL, BD Co.) at a density of 2×10^5 / well. The plates were cultured for 48 h before the experiment.

Before the beginning of the uptake experiment, the cell culture medium was discarded, and the cells were washed three times with 300 μL HBSS (pH 7.4) prewarmed to 37°C. Then 300 μL prewarmed HBSS with/without inhibitors was added to each well, after equilibrating for 15 min, the HBSS in the well was discarded and prewarmed HBSS containing specific substrates and inhibitors was added to each well and incubated at 37°C for the designated time. Then the incubation was stopped by removing the medium and washing the cells three times with ice-cold HBSS. The cells were then lysed by the addition of 200 μL deionized water and freeze-thawed three times. The protein concentration was measured using the BCA assay kit and the cell samples were stored at −20°C until analysis.

Kidney Slices

Kidney slices were assayed as previously described [24]. Rats were sacrificed via exsanguination from the abdominal aorta under anesthesia, and the kidneys were excised. The kidneys were then decapsulated and cored (8 mm i.d.) perpendicular to the corticopapillary axis. Kidney slices with a thickness of 300 mm and a diameter of 8 mm were prepared using a Krumdieck tissue slicer MD6000 (TSE Systems, Chesterfield, MO USA) with ice-cold and carbogen-saturated (95% O_2, 5% CO_2) Krebs-bicarbonate buffer (120 mM NaCl, 16.2 mM KCl, 10 mM Na_2HPO_4/NaH_2PO_4, 1.2 mM $MgSO_4$, and 1 mM $CaCl_2$, pH 7.5) [24]. The tissue slices were pre-incubated in a 24 well plate containing Krebs-bicarbonate buffer under a carbogen-saturated atmosphere at 4 or 37°C for 5 min. Kidney slices were transferred to 24 well-cultured plates containing 1 ml of buffer with test compounds for further incubation at 4 or 37°C. All incubations were under a carbogen atmosphere.

To determine the effect of CRF on the uptake of M20.7, kidney slices from the 5/6 Nx ($n=6$) and control rats ($n=4$) were incubated with 50 or 100 μM M20.7 at 4 or 37°C. The incubation was terminated at 5, 15, and 30 min by removing the slices and rinsing with ice-cold HBSS. To study the effect of uremic toxins on the uptake of M20.7, kidney slices from normal rats were incubated with 100 mM M20.7 in the presence or absence of probenecid and individual or mixed HA and IS with different concentrations for 15 minutes. At the end of each incubation, kidney slices were washed three times with ice-cold HBSS and dried using filter paper. After weighing, each kidney slice was homogenized in 300 mL of saline. M20.7 was determined using LC-MS/MS.

Determination of Uremic Toxins

IS, CMPF, HA, and IAA were determined using a Shimadzu LC-30 AD high-performance liquid chromatography system (Kyoto, Japan) coupled with an API6500 triple-quadrupole mass spectrometer (Applied Biosystems, ON, Canada). Analyst 1.6.2 software (Applied Biosystems) was used for data acquisition and processing and chromatographic separation was achieved on a Venusil ASB-C18 (150 mm × 4.6 mm i.d., 5 mm) at 40°C. The mobile phase was a mixture of 5 mM ammonium acetate (A) and methanol (B) at a flow rate of 0.8 mL/min. The gradient elution program began from 25% B, increased linearly to 90% B in the next 2.7 min, and was maintained for 1.8 min; in the next 1 min, the gradient was reduced to 25% B linearly and was maintained at 25% B until the gradient was stopped at 6 min.

Multiple reaction monitoring (m/z 174.0 → 129.9 for IAA, m/z 178.0 → 133.9 for HA, m/z 212.0 → 131.8 for IS, m/z 239.0 → 194.9 for CMPF, and m/z 136.8 → 92.8 for salicylic acid as internal standard) was used in the negative electrospray ionization mode with an ion spray voltage of −4000 V and a source temperature of 550°C. The nebulizer gas, heater gas, and curtain gas were set to 50, 80, and 25 psi, respectively. The standard curve ranges were 0.100 to 30.0 mM for IAA and CMPF in plasma and 1.00 to 200 mM for IS and HA. The intra- and inter-run precision and accuracy for four uremic toxins from the quality control (QC) samples are summarized in supplemental section (Table S1).

A 25 µL aliquot plasma sample and 25 mL of internal standard (2.00 µg/mL salicylic acid) were mixed with 75 µL of acetonitrile containing 1% formic acid. After vortexing and centrifugation at 14,000 g for 5 min, the supernatants were diluted 4-fold with the initial mobile phase to measure IAA and CMPF by LC-MS/MS; and diluted 40 times to determine HA and IS.

Determination of Vildagliptin and M20.7

Vildagliptin and M20.7 were determined using a Shimadzu LC-30 AD high-performance liquid chromatography system (Kyoto, Japan) coupled with an API5500 triple-quadrupole MS (Applied Biosystems, ON, Canada). Analyst 1.6.2 software (Applied Biosystems) was used for data acquisition and processing. Chromatographic separation was achieved on a HILIC chromatographic column (100 mm × 3.0 mm i.d., 3 µm) at 40°C. The mobile phase was a mixture of 5 mM ammonium acetate containing 0.1% formic acid (A) and methanol (B) at a flow rate of 0.8 mL/min. The gradient elution program began from 90% B, maintained for 0.8 min, and reduced linearly to 75% B over the next 0.5 min, and maintained for 0.9 min; for the next 0.1 min, the gradient was increased to 90% B linearly and maintained at 90% B until the gradient was stopped at 4.2 min.

Multiple reaction monitoring (m/z 304 → 154 for vildagliptin, m/z 323 → 116 for M20.7, m/z 366 → 195 for besigliptin as internal standard of vildagliptin, and m/z 385 → 195 for besigliptin-COOH as internal standard of M20.7) was used in the positive electrospray ionization mode with an ion spray voltage of 4500 V and a source temperature of 500°C. The ion source gas 1, ion source gas 2, and curtain gas were set to 50, 50, and 20 psi, respectively. The standard curve ranges were 2.00 to 1000 ng/mL for vildagliptin and M20.7. The intra- and inter-run precision and accuracy data for the QC samples are exhibited in supplemental section (Table S2).

A 50 µL aliquot of plasma sample and 50 µL of internal standard (10.0 ng/mL of besigliptin and 50.0 ng/mL of besigliptin-COOH) were mixed with 100 µL acetonitrile. The mixture was vortexed for 15 min and centrifuged at 3700 g for 15 min. An aliquot of 10 µL of the resulting supernatant was injected into to LC – MS/MS system for quantitative analysis. The samples exceeding the quantitative upper limit of the standard curve were determined by using a10 times dilution of the blank matrix.

Data Analysis

WinNonlin (version 6.1; Pharsight Corp., Cary, NC) was used to calculate the pharmacokinetic parameters in a noncompartmental model. Maximum plasma concentrations (C_{max}) and their time of occurrence (T_{max}) were determined directly from the observed values. The AUC from time zero to infinity ($AUC_{0-\infty}$) was calculated using the log-linear trapezoidal method. The $t_{1/2}$ was calculated as ln (2)/(slope of the terminal log-linear phase). Systemic clearance (CL) was calculated as dose/$AUC_{0-\infty}$. The apparent volume of distribution (Vss) was determined as CL/(slope of the terminal log-linear phase). GraphPad Prism was used to calculate uptake kinetic parameters and the half inhibitory concentration (IC_{50}). All data were expressed as mean ± standard deviation (S.D.). The student's two-tailed unpaired t-test in SPSS (version 6.0; GraphPad Software, San Diego, CA) was used to determine statistical differences and a $p<0.05$ was considered statistically significant.

The uptake kinetic parameters are fitted and calculated by the folliowing equation using GraphPad Prism (version 6.0; GraphPad Software, San Diego, CA):

$$V = \frac{V_{max\,1} \times S}{K_{m1} + S} + \frac{V_{max\,2} \times S}{K_{m2} + S.}$$

where V, S, K_m and V_{max} represent transport rate (pmol/min/mg protein), substrate concentration (µM) and Michaelis-Menten constant (µM, the substrate concentration when the rate is the half of the maximum rate) and maximum transport rate (pmol/min/mg protein), respectively. OAT3 uptake in OAT3-HEK293 cells was determined after subtracting the uptake by empty-vector transfected cells from total uptake by the OAT3-HEK293.

The substrate uptake rate was normalized using the protein concentration of the cell lysates. The transporter-mediated uptake was obtained by subtracting the accumulation in empty-vector transfected cells from that in the parallel uptake experiments in OAT3-transfected HEK293 cells.

For the inhibition study, IC_{50} values were calculated by plotting the log value of inhibitor concentration against the normalized response as follows:

$$Y(\%) = \frac{1}{1 + 10^{(X - \log IC_{50})}} \times 100\%.$$

Results

Pharmacokinetics of Vildagliptin and M20.7 in Rats

Results of biochemical parameters showed that the 5/6 Nx model was successfully established (Table S3).

After an intragastric administration of 10 mg/kg vildagliptin in control and 5/6 Nx rats, the plasma concentration-time

profiles for vildagliptin and M20.7 are shown in Fig. 2, and the corresponding pharmacokinetic parameters are presented in Table 1. In control rats administrated with vildagliptin, the plasma exposure of the metabolite M20.7 was approximately three times greater than that of the parent drug and similar to that in humans, which also indicated that this was a suitable animal model for investigating the effect of renal insufficiency on the pharmacokinetics of vildagliptin and M20.7.

Compared to the control rats, the C_{max} and $AUC_{0\text{-}t}$ values for vildagliptin in the 5/6 Nx rats increased by 34.0% and 45.8%, respectively. Whereas the C_{max} and $AUC_{0\text{-}t}$ values for M20.7 in the 5/6 Nx rats increased remarkably to 5.20 and 7.51 times that of control. Pharmacokinetic changes of vildagliptin and its metabolites in the 5/6 Nx rats were consistent with those in patients with renal impairment, suggesting that the pharmacokinetics of M20.7 was more affected by renal impairment when compared to those for vildagliptin.

The percentages for the cumulative excretion of vildagliptin and its metabolite M20.7 in urine and feces in both the control and 5/6 Nx groups are shown in Fig. 3. In control rats, the cumulative excretion of vildagliptin in urine and feces within 96 h after dosing, accounted for 16.7% and 19.3% of the administered dose, respectively. The proportions of M20.7 in urine and feces were 43.0% and 8.69%, respectively. Compared with the control group, the urinary and fecal excretion of vildagliptin in the 5/6 Nx rats decreased slightly, from 16.7% to 9.06% and from 19.3%

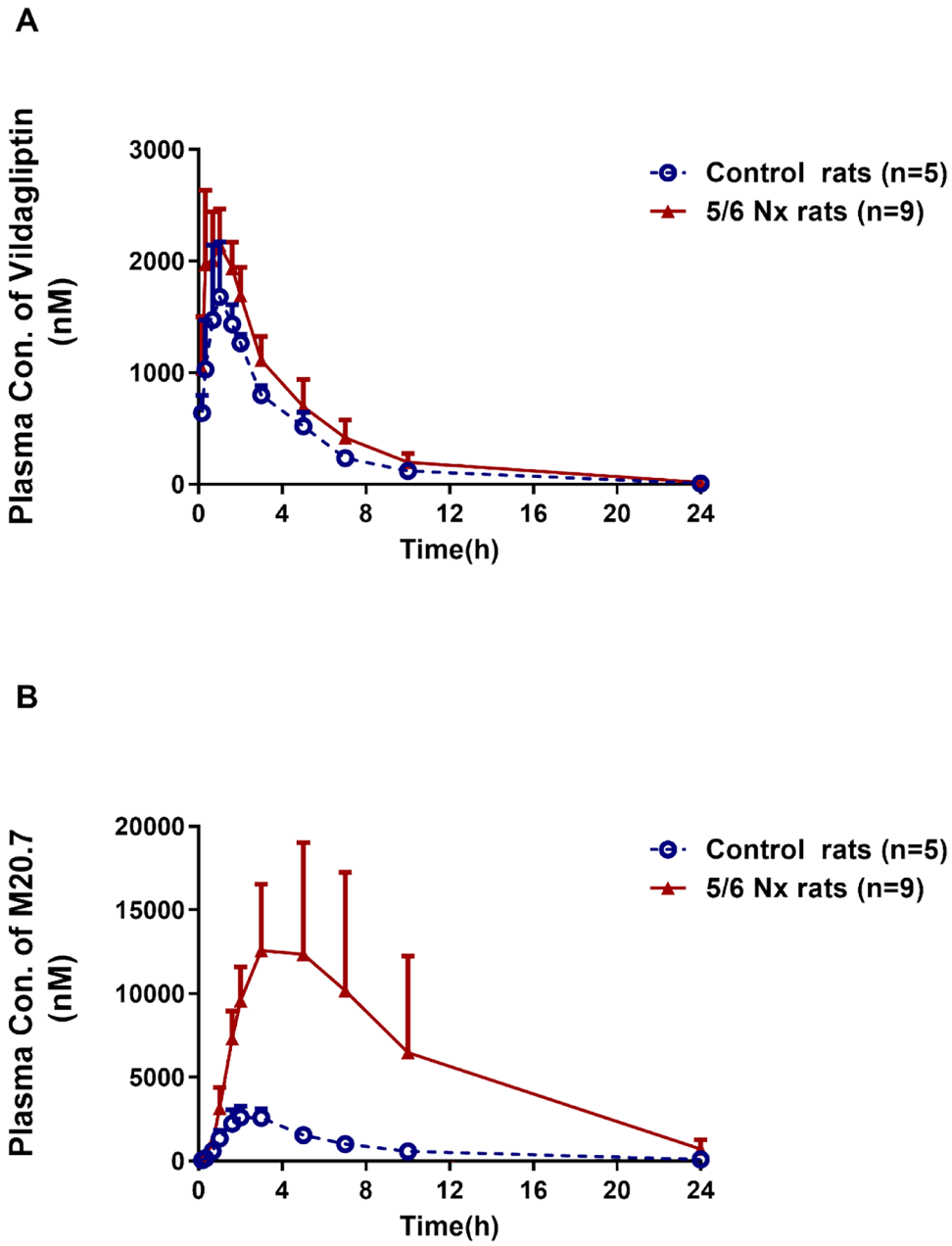

Fig. 2 Mean plasma concentration-time profiles of vildagliptin and M20.7 following an oral administration of vildagliptin (10 mg/kg) to control ($n=5$) and 5/6 Nx ($n=9$) rats. Data are expressed as mean ± SD

Table 1 Pharmacokinetic parameters of vildagliptin and M20.7 after an oral administration of 10 mg/kg vildagliptin to control ($n=5$) and 5/6 Nx ($n=9$) rats

	Vildagliptin		M20.7	
	Control rats ($n=5$)	5/6 Nx rats ($n=9$)	Control rats ($n=5$)	5/6 Nx rats ($n=9$)
C_{max} (μM)	1.75 ± 0.40	2.34 ± 0.36*	2.67 ± 0.56	13.9 ± 5.86**
t_{max} (h)	1.13 ± 0.51	0.95 ± 0.46	2.20 ± 0.45	3.56 ± 1.13*
$t_{1/2}$ (h)	3.13 ± 1.07	3.36 ± 1.35	4.74 ± 1.12	4.32 ± 0.35
AUC_{0-t} (μmol·h/L)	7.12 ± 0.92	10.4 ± 1.8**	18.8 ± 4.3	141 ± 90*
$AUC_{0-\infty}$ (μmol·h/L)	7.15 ± 0.89	10.5 ± 1.9**	19.7 ± 4.0	146 ± 94*
MRT (h)	4.01 ± 0.59	4.22 ± 0.67	7.45 ± 1.97	7.64 ± 1.07

Data are expressed as mean ± SD. * $p<0.05$, ** $p<0.01$, compared with control

to 13.5%, respectively, while the total excretion of urine and feces decreased from 36.0% to 22.6%. Whereas the excretion of M20.7 increased accordingly in 5/6 Nx rats, mainly in the urine, from 43.0% to 58.3% of the dose, suggesting a slight increase in the metabolism of vildagliptin in the 5/6 Nx rats. However, there was no significant difference in the total excretion of urine and feces between the two groups, which was 87.7% for control rats and 92.1% for the 5/6 Nx rats.

Effect of Chronic Renal Impairment on Liver and Kidney Metabolism of Vildagliptin

To evaluate the possible effects of chronic renal impairment on the metabolism of vildagliptin, the differences in the amount of M20.7 formed in the liver and kidney homogenates were evaluated between the two rat groups and the results are shown in Fig. 4. The formation of M20.7 in liver homogenates from the 5/6 Nx rats was significantly higher than that in control rats at 0.05, 0.3 and 2 μM of vildagliptin, and increased by 29.1%, 37.7% and 33.5%, respectively. However, in the renal homogenates from the two groups, there was no significant difference in the formation of M20.7.

Pharmacokinetics of M20.7 after Direct Administration to Rats

To further evaluate whether metabolic differences are responsible for the pharmacokinetic changes in rats with renal impairment, the pharmacokinetics of M20.7 was investigated by intravenous injection. After 1.5 mg/kg M20.7 was injected directly, the mean plasma concentration-time curves in the control and 5/6 Nx rats are displayed in Fig. 5, and the main pharmacokinetic parameters are given in Table 2. Compared to control rats, the total body clearance was significantly slower in the 5/6 Nx rats ($P<0.001$), followed by a 3.34 times increase in the AUC.

Uptake of Vildagliptin and M20.7 by Renal Transporters

The renal clearances of vildagliptin and M20.7 in rats were 2.53 and 5.80 mL/min (GFR = 1.31 mL/min), respectively, which demonstrated that the active secretion may be involved in renal excretion of M20.7. We next evaluated the uptake of M20.7 in renal slices from control and 5/6 Nx rats at 4°C and 37°C (Fig. 6). The uptake from each group of slices at 37°C was significantly higher than that at 4°C. And the uptake of M20.7 in renal slices increased with time at 37°C, but there was no significant difference between the two groups.

To further elucidate the role of renal uptake transporters for the elimination of vildagliptin and M20.7, their uptake by the different renal uptake transporters (OAT1, OAT3 and OCT2)-expressing HEK293 cells were determined and we have previously validated the function of these transporters using typical substrates (PAH for OAT1, E3S for OAT3 and MPP^+ for OCT2, Fig. S1). As shown in Fig. 7, the uptake of vildagliptin was about twice higher in OAT3- and OCT2-transfected cells than in empty-vector transfected cells at 1 and 10 μM, while the uptake of vildagliptin by OAT1-transfected cells was similar to that in the control cells. These data suggested that vildagliptin may be only a weak substrate of OAT3 and OCT2, but not a substrate of OAT1. The uptake of M20.7 was 25.3 and 9.78 times higher, respectively, in OAT3-transfected cells than in empty-vector transfected cells at 1 and 10 μM. The accumulation of M20.7 in OAT1- and OCT2-transfected cells was similar to that in empty-vector-transfected cells. By measuring the time and concentration-dependent uptake of M20.7 by HEK293 cells transfected with OAT3, we further evaluated its role in transport, and the apparent uptake of M20.7 by cells transfected with OAT3 was significantly higher than empty-vector transfected cells at all time points, and increased in a linear time-dependent manner for a 7 min incubation (Fig. S2). Therefore, subsequent concentration-dependent assays were evaluated at 3 min. The Eadie-Hofstee plot (V versus V/S) displayed obvious characteristics of two binding sites (Fig. 8): a high-affinity, low velocity site ($K_{m1}=4.49\pm1.40$ μM, $V_{max1}=8.40\pm1.70$ pmol/min/mg protein) and a low-affinity, high-velocity system ($K_{m2}=127\pm16$ μM, $V_{max2}=185\pm11$ pmol/min/mg protein). Taken together, these results demonstrated that OAT3 was involved in the renal excretion of M20.7.

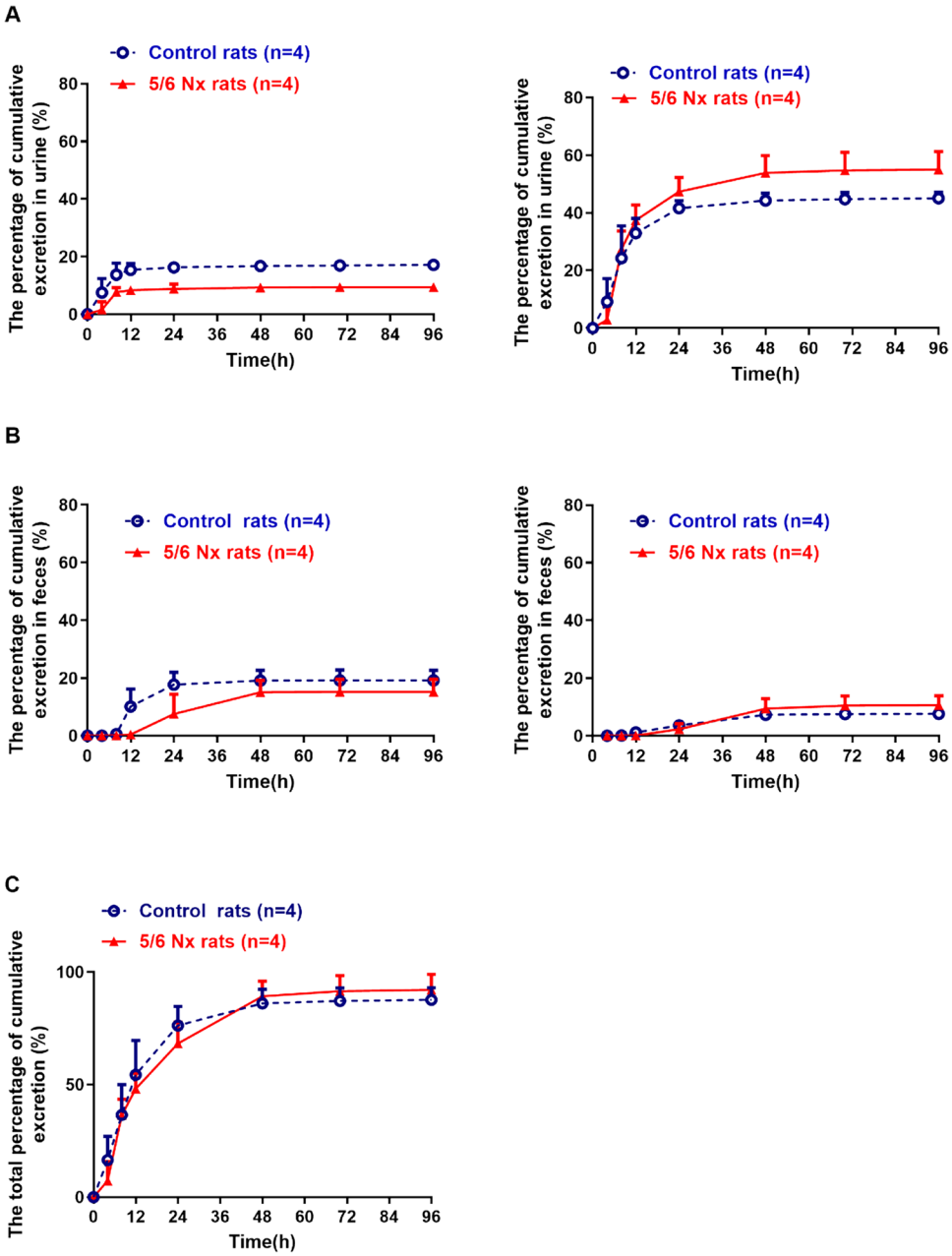

Fig. 3 The percentage of cumulative excretion of vildagliptin (left) and M20.7 (right) in urine (**a**), feces (**b**) and total samples (**c**) after an oral dose of 10 mg/kg vildagliptin to control ($n=4$) and 5/6 Nx ($n=4$) rats. Data are expressed as mean ± SD

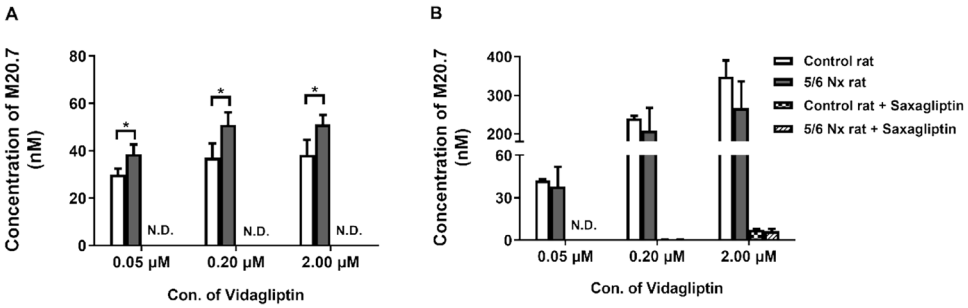

Fig. 4 Comparision of the amounts of M20.7 formed with or without the addition of DPP-IV inhibitor of saxagliptin in liver (**a**) and kidney (**b**) homogenate from control ($n=3$) and 5/6 Nx ($n=3$) rats. Data are expressed as mean ± SD. *, $p<0.05$ compared with control

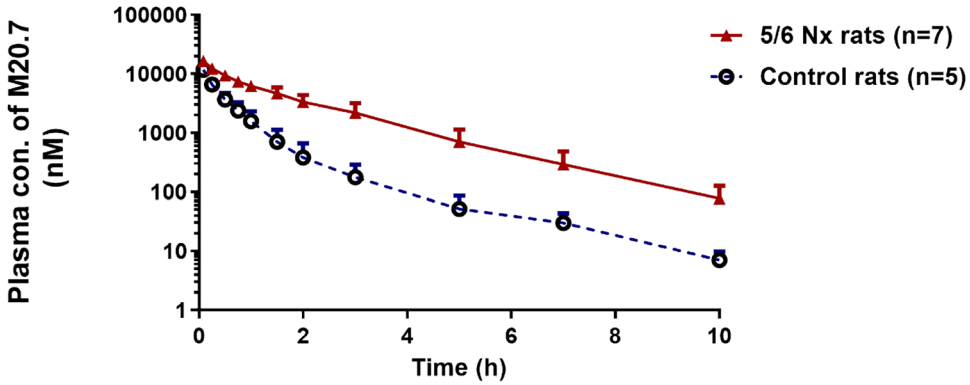

Fig. 5 Mean plasma concentration–time profiles of M20.7 following an intravenous administration of 1.5 mg/kg M20.7 to control ($n=5$) and 5/6 Nx ($n=7$) rats. Data are expressed as mean ± SD

Table 2 Pharmacokinetic parameters of M20.7 after an intravenous administration of 1.5 mg/kg M20.7 to control ($n=5$) and 5/6 Nx ($n=7$) rats

	M20.7	
	Control rats ($n=5$)	5/6 Nx rats ($n=7$)
C_{max} (μM)	11.7 ± 1.1	16.4 ± 1.4***
AUC_{0-t} (μmol·h/L)	6.67 ± 1.83	22.3 ± 5.3***
$AUC_{0-\infty}$ (μmol·h/L)	6.70 ± 1.86	22.4 ± 5.4***
CL (L/h/kg)	0.73 ± 0.18	0.22 ± 0.05***
Vss (L/kg)	1.68 ± 0.44	0.46 ± 0.14***
MRT (h)	0.72 ± 0.15	1.62 ± 0.32***

Data are expressed as mean ± SD. *** $p<0.001$ compared with control

Correlation between the Concentration of Uremic Toxins and Exposure to Vildagliptin and M20.7

Next, the plasma concentrations of the protein-bound uremic toxins CMPF, HA, IS and IAA, that accumulated in the body due to renal impairment was determined. Except for CMPF, which was not detected in rat plasma, the results for the other three uremic toxins IS, HA and IAA are shown in Fig. S3. The plasma concentrations of IS and HA in the 5/6 Nx rats were significantly higher than those in the control rats. After an oral administration of vildagliptin, the correlations between the plasma exposure of vildagliptin and the plasma concentrations of IS, HA and IAA were analyzed. However, a weak correlation was observed with coefficients of 0.6423, 0.5397 and − 0.6300, respectively. Conversely, the increase of AUC_{0-t} for M20.7 was highly correlated with the increase of plasma concentrations of IS and HA, with correlation coefficients of 0.9568 and 0.8974, respectively. There was no significant difference in plasma IAA concentration between the two groups. These results are shown in Fig. 9.

Effect of Uremic Toxins on the Uptake of M20.7

Since the plasma levels of IS and HA in the 5/6 Nx rats were highly correlated with plasma exposure of M20.7, the effect of IS and HA alone or in combination, on the uptake of M20.7 in normal rat kidney slices was investigated (Fig. 10). With an increase in the concentration of uremic toxins, the uptake of M20.7 decreased significantly and when the concentration of IS was set at 50 and 100 μM, the uptake of M20.7 decreased to 83.4% and 72.2% of the control group, respectively. The uptake of M20.7 after the addition of 20, 50 and 100 μM HA, decreased to 89.5%, 79.3% and 70.2% of the control group while the uptake of M20.7 decreased to 93.0%, 78.5% and 62.9% of the control

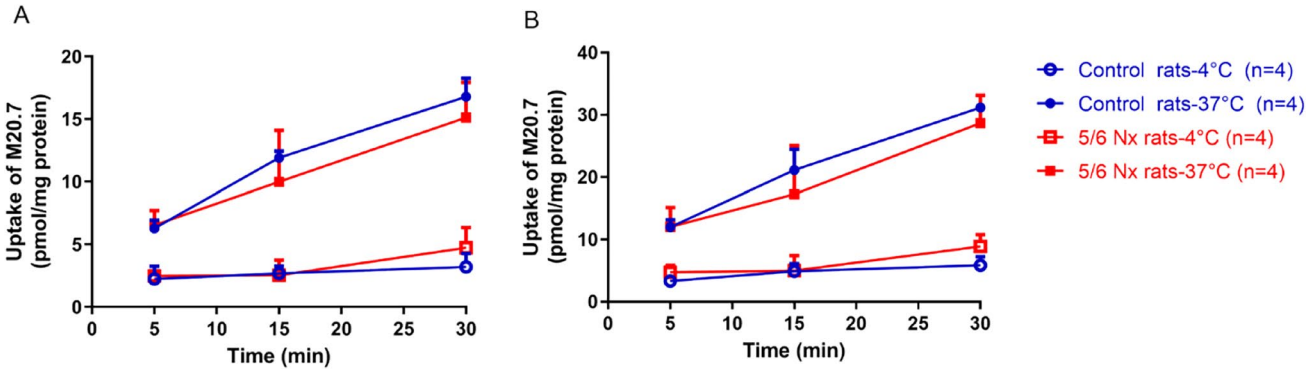

Fig. 6 Uptake of M20.7 in kidney slices of control ($n=4$) and 5/6 Nx ($n=6$) rats at 50 μM (**a**) and 100 μM (**b**). Data are expressed as mean ± SD

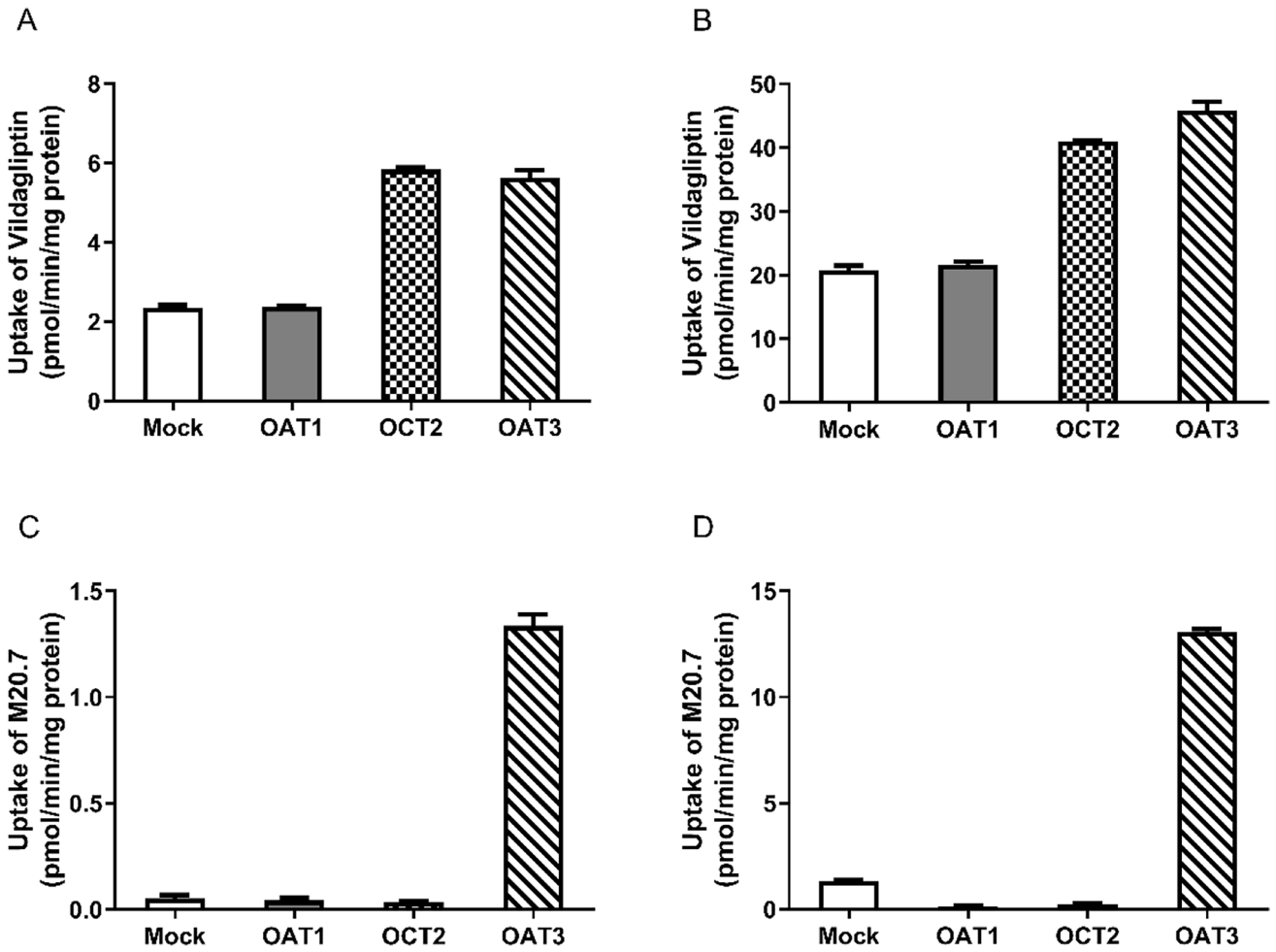

Fig. 7 Uptake of 1 μM vildagliptin (**a**), 10 μM vildagliptin (**b**), and 1 μM M20.7 (**c**), 10 μM M20.7 (**d**) in HEK293-OAT1, HEK293-OAT3, HEK293-OCT2 and HEK293-Mock. Data are expressed as mean ± SD ($n = 3$)

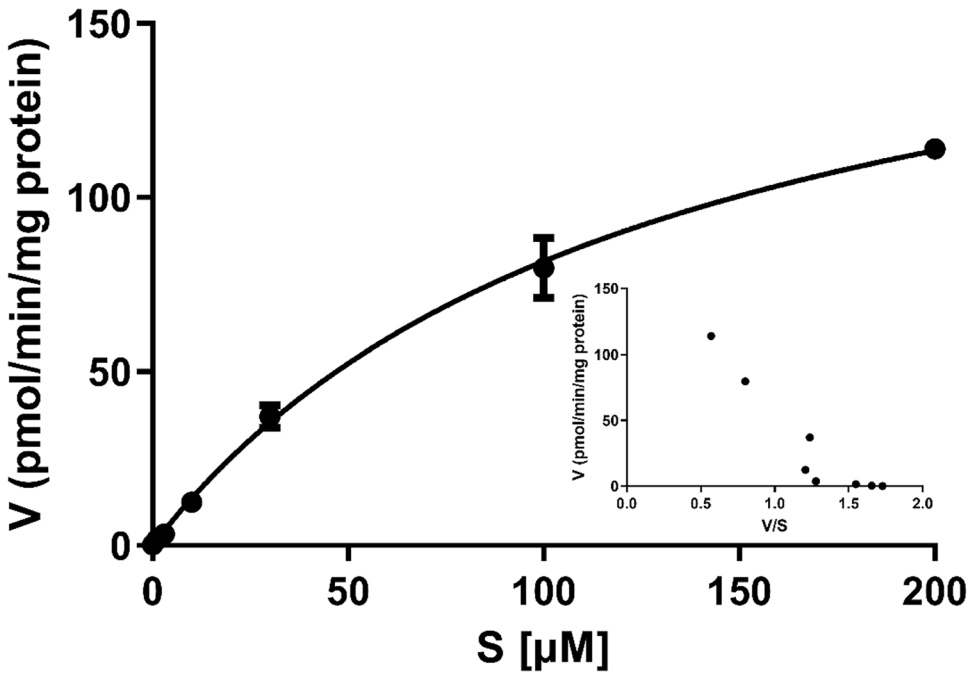

Fig. 8 Concentration dependence of M20.7 uptake by HEK293-OAT3. Data are expressed as mean ± SD ($n = 3$)

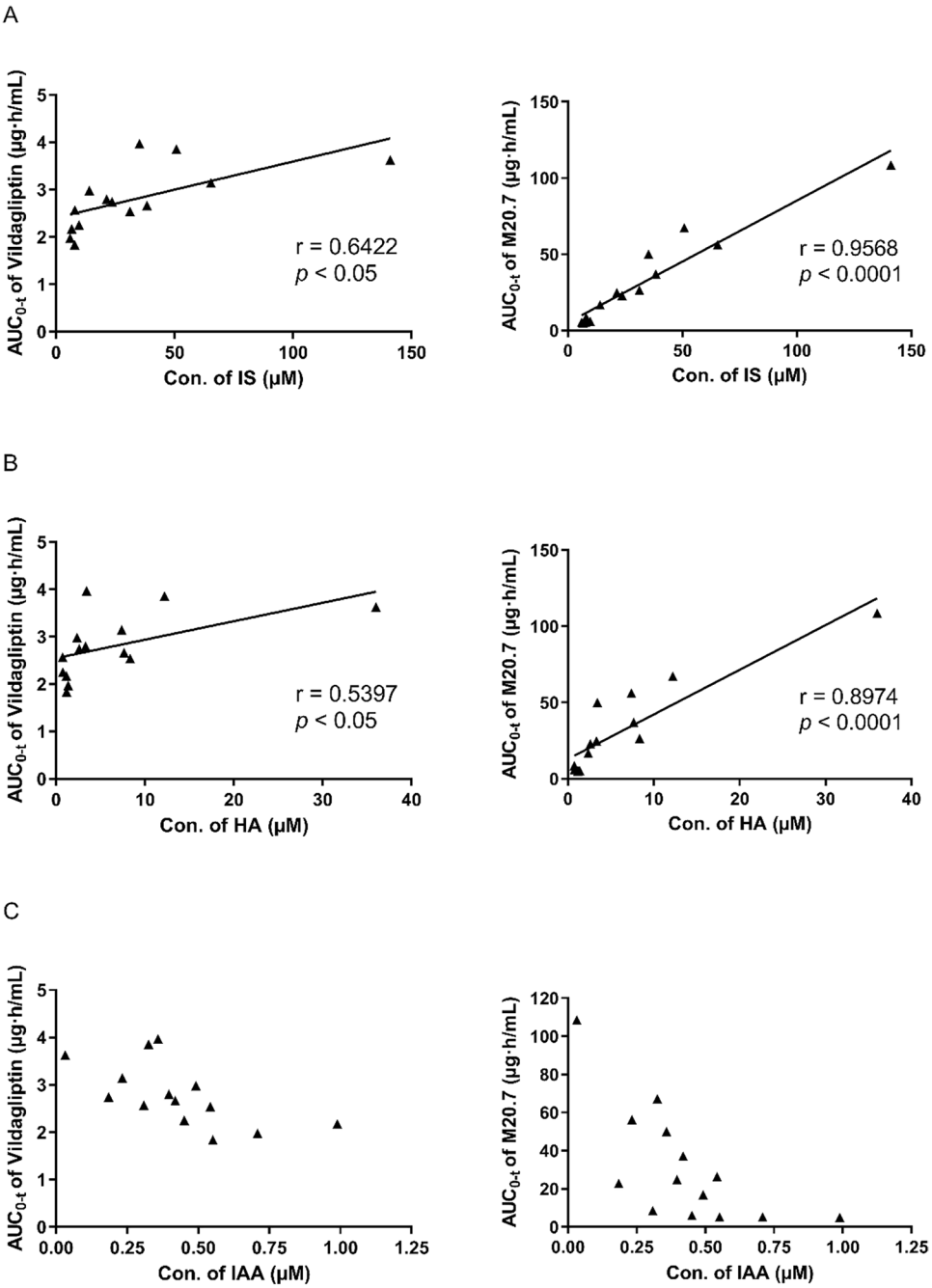

Fig. 9 Correlation between the $AUC_{0\text{-}t}$ values of vildagliptin (left) and M20.7 (right) after an oral dose of vildagliptin and plasma concentrations of IS (**a**), HA (**b**) or IAA (**c**) Data are expressed as mean ± SD ($n = 14$)

group when the concentration of the mixture of IS/HA was 20/20, 50/50 and 100/100 μM, respectively. The inhibitory effect of probenecid, an OAT positive inhibitor, was also investigated and under incubation with 200 and 500 μM probenecid, the uptake of M20.7 decreased to 49.4% and 42.8%, respectively.

The effect of uremic toxins on M20.7 uptake in HEK293 cells overexpressing OAT3 was further investigated and the IC_{50} values for CMPF, HA, IS and IAA on the uptake of M20.7 by OAT3 were 5.75, 29.0, 69.5 and 154 μM, respectively (Fig. 11).

In reference to the proportion of the four uremic toxins accumulated in CRF patients, we investigated the effects of four uremic toxin mixtures on OAT3 uptake. The results showed that a mixture of CMPF, IS, HA and IAA had a strong inhibitory effect on the uptake of M20.7 by OAT3. The lowest concentration (10, 10, 10, 1 μM) of this mixture inhibited the uptake of M20.7 by 63.7% and when the concentration of the mixture increased to 30, 30, 30, 3 μM and above, the inhibition on this uptake was more than 90%, which was similar to the inhibitory effect of OAT3 strong positive inhibitor probenecid (Fig. 11).

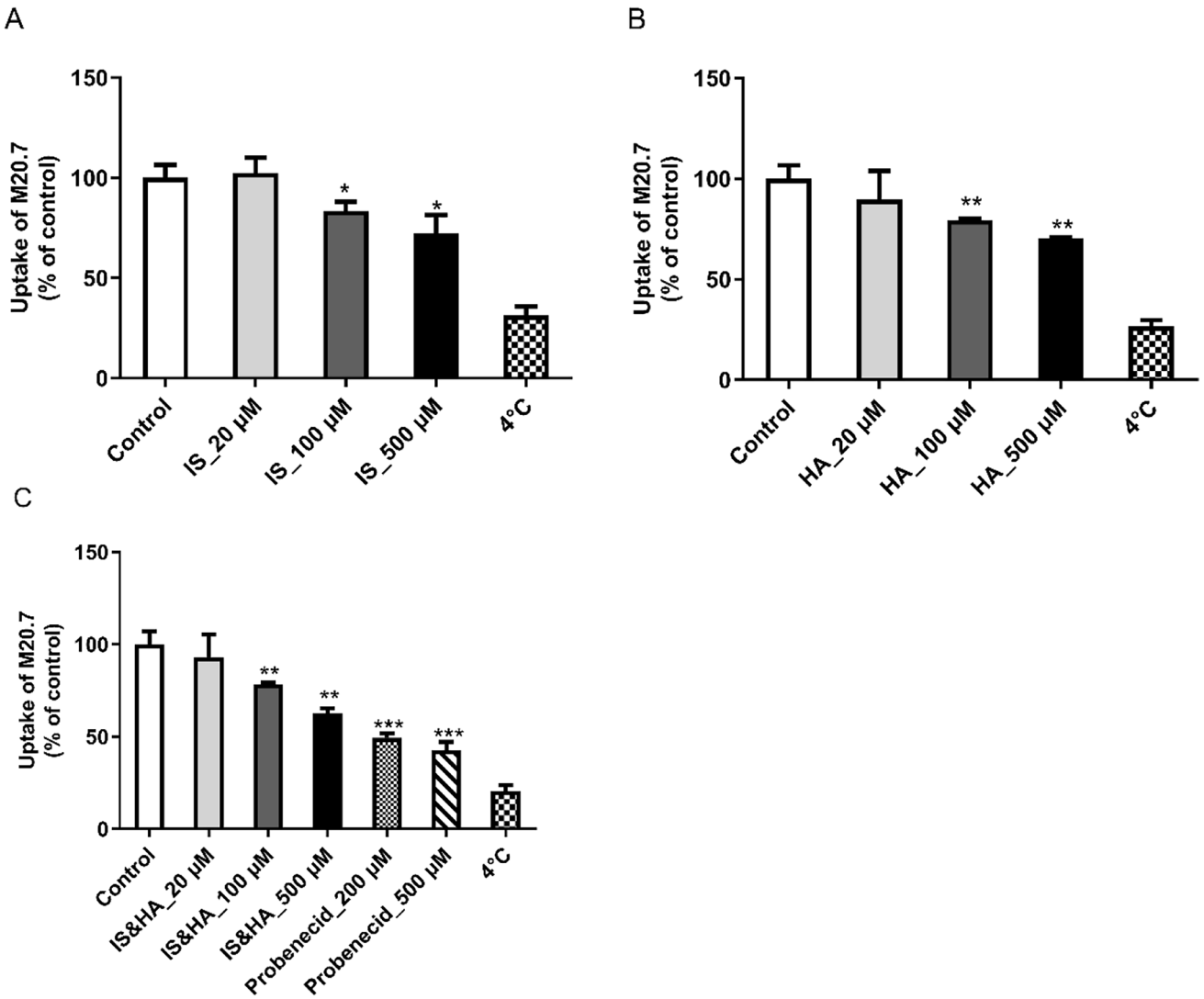

Fig. 10 The inhibitory effect of HA (**a**), IS (**b**) and their mixture (**c**) with different concentration on the uptake of M20.7 in the kidney slices of normal rats. Data are expressed as mean ± SD ($n = 3$).*, $p < 0.05$, **, $p < 0.01$, ***, $p < 0.001$ compared with control

Because CMPF, IS and HA have a strong inhibitory effect on uptake of M20.7 by OAT3, the type of inhibition by the three uremic toxins were investigated and results are shown in Fig. 12. According to the results, it was inferred that the types of inhibition caused by the three uremic toxins were mixed inhibition.

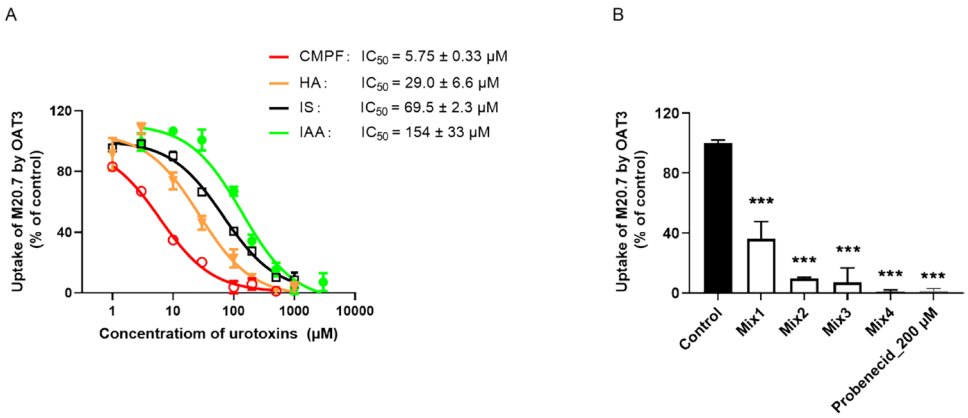

Fig. 11 Inhibitory effects of each four urotoxins (**a**), four urotoxins mixtures and probenecid (**b**) on the M20.7 (30 μM, 3 min) uptake in the OAT3-overexpressed HEK293 cells. Data are expressed as mean ± SD ($n = 3$). ***, $p < 0.001$ compared with control

Discussion

Renal impairment usually alters the plasma exposure of a drug and therefore, when compared to patients with normal renal function, dosage regimens may need to be adjusted for patients with renal impairment. The most common cause of altered pharmacokinetics arising from impaired renal function is a decreased glomerular filtration rate. However, this does not explain why plasma exposure to vildagliptin and its carboxylic acid metabolite M20.7, both excreted by the kidneys, varies so greatly with renal function. In patients with different extents of renal impairment, the AUC for vildagliptin increased by 32% -134%, but the AUC for M20.7 increased by 1.6–6.7 times [6].

Renal impairment can also affect the binding of a drug or its metabolite to plasma proteins, and thus affect their distribution and elimination [25, 26]. However, for drugs with a relatively low plasma protein binding rate (<80%), renal failure will not change its clearance in vivo [27]. The free drug fractions (f_u) of vildagliptin and M20.7 are reported to be 90.3% and 100%, respectively [4]. These results indicated that plasma protein binding abnormalities caused by renal failure have little effect on the altered pharmacokinetics of vildagliptin and its metabolite.

To elucidate the difference in pharmacokinetic changes between vildagliptin and its metabolite in patients with renal impairment, we shifted our focus to the effects of renal failure on metabolism and transport.

In this study, excretion experiments in rats showed that when compared to normal rats, the total excretion of the metabolite M20.7 in the 5/6 Nx group increased by approximately 15% (from 51.7% to 69.5%), and the parent drug decreased by around 13% (from 36.0% to 22.6%). The results of our in vitro experiments also showed that the production of

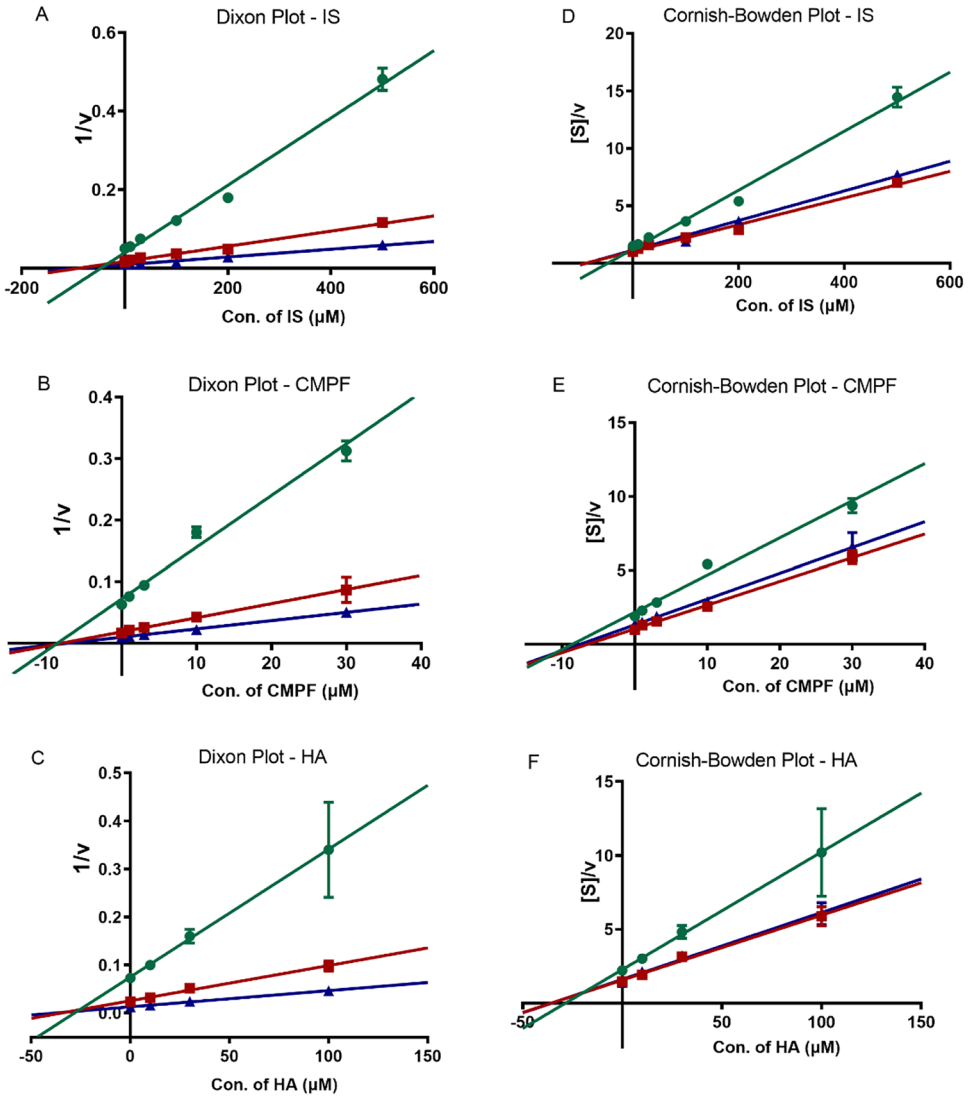

Fig. 12 Dixon plots and Cornish-Bowden plots showing inhibition of the M20.7 by IS, HA and CMPF. Concentrations of M20.7 were 30 μM (●), 60 μM (■), and 130 μM (▲). Data are expressed as mean ± SD ($n = 3$)

M20.7 increased by approximately 30% in the liver homogenates of 5/6 Nx rats. Our previous study revealed that the metabolism of vildagliptin to M20.7 was mainly mediated by DPPs [5]. It has been reported that the activity of DPP-4 in patients with renal failure was slightly increased [28], which may satisfactorily explain the 15% increase in the total recovery of the metabolite M20.7 in the urine and feces of the 5/6 Nx rats. However, the increased proportion was not sufficient to increase the plasma exposure of the metabolite by 1.6 to 6.7 times. When the metabolite was administered intravenously to rats, its plasma exposure remained increased by 3.34-fold in the 5/6 Nx rats, compared to the control group, further demonstrating the contribution of metabolism on the increase of M20.7 exposure in 5/6 Nx rats was limited.

The renal clearance rate of M20.7 in rats was approximately 4.4 times higher than that of GFR, suggesting that there may be active secretion during renal clearance, which we demonstrated in the kidney slice experiments. Further evaluation of the contribution of renal uptake transporters to the renal clearance of M20.7 showed that M20.7 was a two-K_m substrate for OAT3 (K_{m1} = 4.49 μM; K_{m2} = 127 μM), but was not the substrate for OAT1 or OCT2. Moreover, it is the low-K_m site of M20.7 uptake by OAT3 that is likely to be relevant clinically, since in patients with normal renal function, the plasma level of M20.7 was about 0.76 μM at regular doses of vildagliptin (50 mg twice daily) [4]. The uptake fold of vildagliptin by OAT3 and OCT2 was close to the threshold (2 times) of the substrate judgment criteria recommended by the US FDA [29]. In addition, following oral administration, vildagliptin was rapidly and well absorbed with an absolute bioavailability of 85%, indicating that vildagliptin has high permeability. Therefore, the effect of transporters on distribution and excretion of vildagliptin might be ignored. It is speculated that the increased exposure of M20.7 in the plasma of patients with renal failure may be related to the change in OAT3 activity, while the decrease in the renal clearance rate of vildagliptin may be related to the decrease in glomerular filtration rate.

Previous results from our laboratory have shown that the mRNA expression of Oat3 in the kidney of rats from the 5/6 Nx group was significantly decreased to approximately 50% of that in the control group, but the transporter activity was not affected [13]. Our current experiment with kidney slices also demonstrated no significant difference in the renal uptake activity of M20.7 between the two groups. The uremic toxins CMPF, HA, IS and IAA, that accumulate in renal impairment patients, could inhibit the uptake of N^+-glucuronides and sulfate conjugates of morinidazole by OAT3 [13]. Therefore, the effects of these uremic toxins on the renal uptake of M20.7 were evaluated. The results showed that CMPF, HA and IS had the greatest inhibitory effect on M20.7 uptake, with an IC_{50} value of 5.75, 29.0 and 69.5 μM, which were dramatically lower than their average concentrations found in the plasma of patients with renal impairment [15]. In addition, the IC_{50} value of IAA for the uptake of M20.7 by OAT3 was 154 μM, which was higher than its plasma concentration in patients with renal failure (5 μM), indicating that its effect on M20.7 in vivo was limited [15]. To simulate the inhibition of uremic toxins on OAT3 in vivo, we investigated the effect of a mixture of four uremic toxins on the uptake of M20.7 by OAT3. The proportion of the four mixed uremic toxins was based on their average plasma concentration in patients with renal impairment and results showed that the inhibitory effect of these mixed uremic toxins at the lowest concentration (Mix1) could reach more than 50%, and other Mixes 2–4 almost completely inhibited the uptake process, like the inhibitory effect seen by application of probenecid, a strong positive inhibitor of OAT3.

The type of inhibition caused by IS, CMPF and HA on the uptake of M20.7 by OAT3 was further investigated. According to the characteristics from the Dixon plot, it can be seen that the type of inhibition with the three inhibitors is competitive or mixed inhibition, rather than non-competitive inhibition [30]. Furthermore, based on the Corish-Bowden plot, the inhibition type of the three uremic toxins was mixed inhibition [31]. Previous studies have reported that IS and CMPF are substrates for OAT3, and our laboratory has also shown that HA is also a substrate for OAT3 (Data not presented). Theoretically, they would have a competitive inhibitory effect on M20.7, suggesting that these uremic toxins have other inhibitory effects on the transporter itself, which need further investigation.

Although it is uncertain whether adverse effects of vildagliptin are associated with high plasma exposure of M20.7, it is recommended that the dose of vildagliptin be halved for patients with moderate and severe renal impairment [28]. In addition, unlike M20.7, most carboxylic acid-containing drugs or metabolites tend to form reactive, electrophilic acyl glucuronides in vivo, which could cause toxic reactions through different mechanisms. For example, the acyl glucuronide metabolite of gemfibrozil might cause rhabdomyolysis, due to the potent inhibition of CYP2C8 [32]. Hepatotoxicity induced by nonsteroidal anti-inflammatory drugs (NSAIDs) may be associated with the covalent binding of their acyl glucuronic acid conjugates to proteins [33]. Therefore, it is of great clinical significance to study the pharmacokinetic characteristics and mechanism of action of carboxylic acid drugs and metabolites in different populations, to provide a theoretical basis for the formulation of drug administration regimens and the prediction of adverse reactions.

Conclusion

To sum up, due to the decrease of glomerular filtration rate in patients with renal impairment, the plasma exposure of vildagliptin increased from 32% to 134%. And at the same time, there was inhibition of OAT3 activity by the

accumulated uremic toxins CMPF, HA, and IS in vivo, leading to blockage of the renal excretion of M20.7 (substrate of OAT3). This causes an increase in plasma exposure by 1.6–6.7 times. In addition, the slight increase in DPPs activity in patients with renal impairment has a limited effect on the plasma exposure to the metabolite of vildagliptin.

Supplementary Information The online version contains supplementary material available at https://doi.org/10.1007/s11095-022-03324-9.

Acknowledgments This study was supported by the National Natural Science Foundation of China (Grant 82073924). The authors thank Xiao-yan Pang for her assistance with the experiments.

Author Contribution ZTG, FDK and XYC participated in research design; ZTG, FDK, NJX, ZDC and JFH performed experiments; ZTG and XYC wrote the manuscript.

Declarations

Conflict of Interest The authors declare no conflict of interest.

References

1. Villhauer E. 1-[[(3-hydroxy-1-adamantyl) amino] acetyl]-2-cyano-(s)-pyrrolidine : a potent, selective, and orally bioavailable dipeptidyl peptidase iv inhibitor with antihyperglycemic properties. J Med Chem. 2003;46(13):2774–89.
2. Mentlein R. Dipeptidyl-peptidase iv (cd26)--role in the inactivation of regulatory peptides. Regul Pept. 1999;85(1):9–24. https://doi.org/10.1016/s0167-0115(99)00089-0.
3. Kreymann B, Williams G, Ghatei MA, Bloom SR. Glucagon-like peptide-1 7-36: a physiological incretin in man. Lancet. 1987;2(8571):1300–4. https://doi.org/10.1016/s0140-6736(87)91194-9.
4. He H, Tran P, Yin H, Smith H, Batard Y, Wang L, et al. Absorption, metabolism, and excretion of [14c]vildagliptin, a novel dipeptidyl peptidase 4 inhibitor, in humans. Drug Metab Dispos. 2009;37(3):536–44. https://doi.org/10.1124/dmd.108.023010.
5. Kong FD, Pang XY, Zhao JH, Deng P, Zheng MY, Zhong DF, et al. Hydrolytic metabolism of cyanopyrrolidine dpp-4 inhibitors mediated by dipeptidyl peptidases. Drug Metab Dispos. 2019;47(3):238–48. https://doi.org/10.1124/dmd.118.084640.
6. He Y. Clinical pharmacokinetics and pharmacodynamics of vildagliptin. Clin Pharmacokinet. 2012;51(3):147–62.
7. Scheen AJ. Pharmacokinetics of dipeptidylpeptidase-4 inhibitors. Diabetes Obes Metab. 2010;12(8):648–58. https://doi.org/10.1111/j.1463-1326.2010.01212.x.
8. Lukashevich V, Schweizer A, Shao Q, Groop PH, Kothny W. Safety and efficacy of vildagliptin versus placebo in patients with type 2 diabetes and moderate or severe renal impairment: a prospective 24-week randomized placebo-controlled trial. Diabetes Obes Metab. 2011;13(10):947–54. https://doi.org/10.1111/j.1463-1326.2011.01467.x.
9. Disease K. Improving global outcomes (kdigo) ckd work group. Kdigo 2012 clinical practice guideline for the evaluation and management of chronic kidney disease. Pol Arch Med Wewn. 2013;120(7–8):300–6.
10. Periclou A, Ventura D, Rao N, Abramowitz W. Pharmacokinetic study of memantine in healthy and renally impaired subjects. Clin Pharmacol Ther. 2006;79(1):134–43.
11. Asconapé JJ. Use of antiepileptic drugs in hepatic and renal disease. Handb Clin Neurol. 2014;119(119):417–32.
12. Zhong K, Li X, Xie C, Zhang Y, Zhong D, Chen X. Effects of renal impairment on the pharmacokinetics of morinidazole: uptake transporter-mediated renal clearance of the conjugated metabolites. Antimicrob Agents Chemother. 2014;58(7):4153–61. https://doi.org/10.1128/aac.02414-14.
13. Kong F, Pang X, Zhong K, Guo Z, Li X, Zhong D, et al. Increased plasma exposures of conjugated metabolites of morinidazole in renal failure patients: a critical role of uremic toxins. Drug Metab Dispos. 2017;45(6):593–603. https://doi.org/10.1124/dmd.116.074492.
14. Chu X, Bleasby K, Chan GH, et al. The complexities of interpreting reversible elevated serum creatinine levels in drug development: does a correlation with inhibition of renal transporters exist? Drug Metab Dispos. 2016;44(9):1498.
15. Vanholder R, De Smet R, Glorieux G, Argiles A, Baurmeister U, Brunet P, et al. Review on uremic toxins: classification, concentration, and interindividual variability. Kidney Int. 2003;63(5):1934–43. https://doi.org/10.1046/j.1523-1755.2003.00924.x.
16. Hsueh CH, Yoshida K, Zhao P, Meyer TW, Zhang L, Huang SM, et al. Identification and quantitative assessment of uremic solutes as inhibitors of renal organic anion transporters, oat1 and oat3. Mol Pharm. 2016;13(9):3130–40.
17. Kearney BP, Yale K, Shah J, Zhong L, Flaherty JF. Pharmacokinetics and dosing recommendations of tenofovir disoproxil fumarate in hepatic or renal impairment. Clin Pharmacokinet. 2006;45(11):1115–24.
18. Anderson S, Rennke HG, Brenner BM, Anderson S, Meyer TW, Rennke HG, et al. Control of glomerular hypertension limits glomerular injury in rats with reduced renal mass. J Clin Investig. 1985;76(2):612–9.
19. Kikuchi K, Itoh Y, Tateoka R, Ezawa A, Murakami K, Niwa T. Metabolomic analysis of uremic toxins by liquid chromatography/electrospray ionization-tandem mass spectrometry. J Chromatogr B Anal Technol Biomed Life Sci. 2010;878(20):1662–8.
20. Naud J, Michaud J, Beauchemin S, Hebert MJ, Roger M, Lefrancois S, et al. Effects of chronic renal failure on kidney drug transporters and cytochrome p450 in rats. Drug Metab Dispos. 2011;39(8):1363–9. https://doi.org/10.1124/dmd.111.039115.
21. Deguchi T, Nakamura M, Tsutsumi Y, Suenaga A, Otagiri M. Pharmacokinetics and tissue distribution of uraemic indoxyl sulphate in rats. Biopharm Drug Dispos. 2010;24(8):345–55.
22. Kaplan MM, Utiger RD. Iodothyronine metabolism in liver and kidney homogenates from hyperthyroid and hypothyroid rats. Endocrinology. 1978;103(1):156–61. https://doi.org/10.1210/endo-103-1-156.
23. Han YH, Busler D, Hong Y, Tian Y, Chen C, Rodrigues AD. Transporter studies with the 3-o-sulfate conjugate of 17alpha-ethinylestradiol: assessment of human kidney drug transporters. Drug Metab Dispos. 2010;38(7):1064–71. https://doi.org/10.1124/dmd.109.031526.
24. Obatomi DK, Brant S, Anthonypillai V, Early DA, Bach PH. Optimizing preincubation conditions for precision-cut rat kidney and liver tissue slices: effect of culture media and antioxidants. Toxicol in Vitro. 1998;12(6):725–37. https://doi.org/10.1016/S0887-2333(98)00055-1.
25. Keller F, Maiga M, Neumayer HH, Lode H, Distler A. Pharmacokinetic effects of altered plasma protein binding of drugs in renal disease. Eur J Drug Metab Pharmacokinet. 1984;9(3):275–82.
26. Reidenberg MM, Drayer DE. Alteration of drug-protein binding in renal disease. Clin Pharmacokinet. 1984;9(1 Supplement):18.
27. FDA. Guidance for industry pharmacokinetics in patients with impaired renal function – study design, data analysis, and impact

on dosing, U.S. Department of health and human services food and drug administration center for drug evaluation and research (cder). 2020.
28. He YL, Kulmatycki K, Zhang YM, Zhou W, Reynolds C, Ligueros-Saylan M, et al. Pharmacokinetics of vildagliptin in patients with varying degrees of renal impairment. Int J Clin Pharmacol Ther. 2013;51(9):693–703. https://doi.org/10.5414/cp201885.
29. FDA. In vitro drug interaction studies —cytochrome p450 enzyme and transporter mediated drug interactions-guidance for industry. 2020.
30. Dixon M. The determination of enzyme inhibitor constants. Biochem J. 1953;55(1):170–1. https://doi.org/10.1042/bj0550170.
31. Cornish-Bowden A. A simple graphical method for determining the inhibition constants of mixed, uncompetitive and non-competitive inhibitors. Biochem J. 1974;137(1):143–4.
32. Ogilvie BW. Glucuronidation converts gemfibrozil to a potent, metabolism-dependent inhibitor of CYP2C8: implications for drug-drug interactions. Drug Metab Dispos. 2005;34(1):191–7.
33. Bailey MJ, Dickinson RG. Acyl glucuronide reactivity in perspective: biological consequences. Chem Biol Interact. 2003;145(2):117–37. https://doi.org/10.1016/s0009-2797(03)00020-6.